Flame Retardance and Mechanical Properties of a Polyamide 6/Polyethylene/Surface-Modified Metal Hydroxide Ternary Composite via a Master-Batch Method

Shu-Mei Liu,[1] Jun-Yi Huang,[1] Zhi-Jie Jiang,[1] Chen Zhang,[1] Jian-Qing Zhao,[1] Jun Chen[2]

[1]*College of Materials Science and Engineering, South China University of Technology, 510640 Guangzhou, China*
[2]*Key Laboratory of Guangdong for High Property and Functional Macromolecular Materials, South China University of Technology, 510640 Guangzhou, China*

Received 16 March 2009; accepted 30 December 2009
DOI 10.1002/app.32086
Published online 12 May 2010 in Wiley InterScience (www.interscience.wiley.com).

ABSTRACT: Surface-modified aluminum hydroxide and magnesium hydroxide mixtures (SAMHs) were filled with linear low-density polyethylene (LLDPE) with a maleic anhydride grafted polyethylene (PE) compatibilizer to produce a SAMH master batch, which was then dispersed in polyamide 6 (PA6) to yield a PA6/PE/SAMH (50/20/30 by weight ratio) ternary composite. Through such a master-batch method, an effective flame retardance UL94 V-0 rating at a 3.2 mm thickness with a 33% limiting oxygen index was achieved. The flame-retardance mechanism of the ternary composite was investigated by thermogravimetric analysis and scanning electron microscopy/energy dispersive X-ray spectroscopy analysis. A cocontinuous PA6/PE polymer host and a preferential dispersion of SAMH particles in the matrix induced the formation of a compact flame-resistant char layer and a high residue rate during burning; this resulted in the desired flame retardance of the ternary composite. © 2010 Wiley Periodicals, Inc. J Appl Polym Sci 117: 3370–3378, 2010

Key words: dispersions; flame retardance; polyamides; polyethylene (PE)

INTRODUCTION

Polyamide 6 (PA6) is one of the most commonly used engineering plastics in industrial applications. The properties of PA6, such as rigidity and processing characteristics, can be improved by small additions of linear low-density polyethylene (LLDPE). PA6/LLDPE blends[1,2] and their complex composites[3] containing short-fiber reinforcements have also been studied thoroughly because of their potential to obtain desired properties. PA6/LLDPE blends are considered to be more combustible than PA6 because of the high flammability of LLDPE. Various stringent flame-retardance standards for plastics in electrical and electronic device fields are required for compliance, but fewer studies have been published on the flame-retardance improvement of PA6/LLDPE blends.

Metal hydroxides, notably, aluminum hydroxide (ATH) and magnesium hydroxide (MH), are perhaps the most environmentally friendly flame retardants used in individual polyethylene (PE)[4] and PA6.[5,6] Moreover, they can fill and strengthen to some degree two kinds of plastics. However, the flame retardance effects of ATH and MH on PA6/LLDPE blends have not been studied, possibly because of their evident drawbacks, such as a poor interface interaction and the rather large amount of ATH and MH (50–65 wt %) needed; these negatively affect the rheological properties and impact toughness of the plastics. Silane coupling agents are usually designed as molecular bridges to modify the interaction between polymer matrices and metal hydroxide surfaces,[7] whereas phosphorus additives have been found to be synergistic flame retardants with metal hydroxides in many polymers.[8] Therefore, it is believed that metal hydroxides coated by silane coupling agents containing phosphorus can facilitate compounding with PA6/LLDPE blends and afford acceptable flame retardance because of a synergistic effect between phosphorus and silicon. In addition, boric compounds are speculated to intensify the dehydration processes advantageous for charring and are used to meet the demand of high-performance engineering plastics. However, boric compounds are incompatible with the polymer matrix and their inclusion usually causes further

Correspondence to: S.-M. Liu (liusm@scut.edu.cn) or J.-Q. Zhao (psjqzhao@scut.edu.cn).

Contract grant sponsor: Specialized Research Fund for the Doctoral Program of Higher Education; contract grant number: 200805611098.

Contract grant sponsor: Key Project for High and New Technology Area of Guangdong Province; contract grant number: 2007A010500001.

deterioration of the mechanical and processing properties of plastics. Synergism between boron and phosphorus found from char measurements showed that a comparable product containing only phosphorus gave less char than the product containing both phosphorus and boron elements.[9]

γ-Diethoxyphosphorous ester propyldiethoxymethylsilane (γ-PSi) is a kind of silane coupling agent containing the phosphorus element. In this study, three synergistic co-additives, boric acid, γ-PSi, and diphenylsilanediol coupling agents, were jointly used to modify a mixture of ATH and MH (2 : 1 by weight ratio) in a surface-modified process.[10] The surface-modified ATH and MH mixtures (SAMHs) simultaneously exhibited favorable flame retardance on the PA6/LLDPE blends because of the synergistic effect between the metal hydroxides and boron, phosphorus, and silicon elements and enhanced interfacial adhesion with polymer matrix due to an organic coating layer of inorganic flame retardants. It is well known that a master-batch processing strategy is helpful to the dispersion of inorganic particles in a polymer matrix.[11] Here, SAMH was first filled with LLDPE with a maleic anhydride grafted polyethylene (PE-*g*-MAH) compatibilizing agent to prepare an SAMH master batch with a filler content of 50 wt % by melt blending. Then, the resultant SAMH master batch was dispersed in the PA6 matrix to form PA6/PE/SAMH (where PE refers to LLDPE and PE-*g*-MAH) ternary composite at a 50/20/30 weight ratio. An additional, significant improvement in the flame retardance of the PA6/LLDPE blend was found, and a UL94 V-0 rating at 3.2 mm of thickness was passed at only a 30 wt % SAMH loading via the master-batch method. Here, LLDPE played the role of increasing the viscosity and decreasing the dripping of the formed ternary composite. However, excellent flame retardance could not be achieved by a direct melt-extrusion process of PA6, PE, and SAMH under the same conditions. The flame-retarded ternary composite met well the growing industrial demand to develop halogen-free solutions in terms of fire protection.

EXPERIMENTAL

Materials

MH (Martifin H-5, d_{90} (The diameter of 90% particles) = 2.4–4.4 μm) and ATH (MARTINAL OL-107LE, d_{90} = 1.5–3.5 μm) were supplied by Martinswerk GmbH (Germany). LLDPE (trade name 7042, density = 0.918–0.935 g/cm^3, melt flow rate = 2.0 g/10 min, 2.16 kg, 190°C) was provided by Sinopec Maoming Refining and Chemical Co., Ltd. (China) and was used as received. PA6 was M32800 (density = 1.13 g/cm^3) from Guangdong Xinhui Meida Nylon Co., Ltd., and was carefully dried *in vacuo* at 90°C for 6 h before mixing. PE-*g*-MAH came from Uniroyal Chem (maleic anhydride content = 1.2 wt %, melt flow rate = 19.8 g/10 min, 2.16 kg, 190°C) and was kept in a vacuum oven at 65°C for 8 h. Diphenylsilanediol was delivered by Bluestar New Chemical Material Co., Ltd., and Jiangxi Xinghuo Organicsilcone Plant (China). Boric acid, dibutyl tin dilaurate, methanol, and xylene were obtained from Tianjin Fuyu Chemical Co. (China). The molecular formula of γ-PSi is

It was synthesized according to Oliver's[12] patent (P content = 10%, Si content = 9%).

Surface modification of maleic anhydride

ATH (100 g) and 50 g of MH were dispersed in 500 mL of xylene under mechanical agitation, then was heated to 140°C. γ-PSi (3.7 g), boric acid (0.8 g), diphenylsilanediol (0.5 g), and dibutyl tin dilaurate (0.05 g) were in turn charged into the system. After the mixture was stirred and refluxed for 6 h, xylene was vacuum-distilled off, and the residue was washed with methanol several times and dried at 80°C *in vacuo* for 20 h to give a white powder product called SAMH.

Preparation of the composites

Two kinds of PA6/PE/SAMH ternary composites were produced by two different processing procedures. A one-shot method was the mixture of 500 g of PA6, 150 g of LLDPE, 50 g of PE-*g*-MAH, and 300 g of SAMH was directly melt-kneaded and extruded in a 30-mm twin-screw extruder at a cylinder temperature of 200–230°C, and the obtained ternary composite was named PAEAM1. A master-batch method (i.e., a two-step blending sequence) was included: the mixture of 375 g of LLDPE, 125 g of PE-*g*-MAH, and 500 g of SAMH were extruded at a cylinder temperature of 180–200°C in the first step, and the obtained composite was called the SAMH master batch; then, a mixture of 500 g of PA6, 400 g of the SAMH master batch, and 100 g of SAMH was subsequently melt-kneaded and extruded into pellets at a cylinder temperature of 200–230°C in the second step, and the obtained ternary composite was named PAEAM2. The weight ratio of PA6/LLDPE/PE-*g*-MAH/SAMH was 50/15/5/30 in both composites. The resulting pellets were dried at 80°C for 5 h and then injection-molded at an injection temperature of 200–235°C into test pieces.

The PA6 composite with 50 wt % SAMH (PASA) was prepared by the compounding of 500 g of PA6

and 500 g of SAMH in a 30-mm twin-screw extruder at a cylinder temperature of 210–240°C, and the LLDPE composite with 50 wt % SAMH (PESA) was obtained via the compounding of 500 g of LLDPE and 500 g of SAMH at a cylinder temperature of 175–200°C. The resulting PASA pellets were dried at 90°C for 8 h and then injection-molded at an injection temperature of 210–245°C into test pieces. The resulting PESA pellets were dried at 70°C for 8 h and then injection-molded at an injection temperature of 180–210°C into test pieces.

All test pieces were conditioned to individual standard status before measurement of the flame-retardance and mechanical properties.

Characterization

The limiting oxygen index (LOI) was tested by an oxygen index/FTA instrument (Fire Testing Technology Co., Ltd., England) according to ASTM 2863-98. Additionally, the vertical burning test was carried out with a UL94 flammability meter (Fire Testing Technology Co., Ltd.) according to UL94 classification. The impacting fracture section of the specimens and the residue of UL94 test coated with ultrathin gold were observed on a JSM-6380 scanning electron microscope/energy dispersive X-ray analyzer (JEOL, Japan). Different area morphologies of the sample were investigated with scanning electron microscopy (SEM), and the elemental distribution was examined by element mapping and point analyses with energy-dispersive X-ray spectroscopy (EDX). The morphology of SAMH particles was examined from the product powder dispersed in ethanol by SEM. Thermogravimetric analysis (TGA) was performed on a TG 209 F1 thermogravimetric analyzer (Netzsch-Gerätebau GmbH, Germany) from 30 to 600°C at a heating rate of 20°C/min under a nitrogen flow.

According to the ASTM D 638 standard, the tensile strength of the specimens was determined with a AG-1 universal electronic tensile testing machine (Shimadzu, Japan). The flexural strength was determined according to ASTM D 790. The Izod impact strength of the notched specimen was determined with a Zwick 5102 pendulum type testing machine (Zwick/Roell, German) according to ASTM D 256.

RESULTS AND DISCUSSION

Flame retardance of the PA6/PE/SAMH composites

Good flame retardance of SAMH on LLDPE due to the introduction of synergistic B, P, and Si elements from boric acid, γ-PSi, and diphenylsilanediol co-additives was reported in our early article, and PESA presented the V-1 rating at a 3.2-mm thickness with a 32% LOI value.[10] The effect of SAMH on the flame retardance of the PA6 and PA6/LLDPE blends was investigated. PA6 was flammable, and its LOI value reported in the literature usually varies in the range 23–27% with a V-2 rating. An increase in the SAMH amount led to an increase in the LOI value and helped with the attainment of a V-0 rating in many cases with two kinds of material. The UL94 ratings of PA6 strongly depends on the tendency for the polymer to drip. The main problem encountered with the compounding of MH and ATH into PA6 is the partial degradation of the polymer,[5] which reduces the viscosity and increases dripping. A large amount of SAMH is required for a satisfying flame-retardance rating of PA6. The PA6 composite with 30 wt % SAMH dripped severely during the test, and a 50 wt % SAMH loading was needed for PA6 to pass the V-0 rating at a 3.2-mm thickness. The LOI and UL-94 test results of PASA and PESA are listed in Table I.

TABLE I
LOI Values and UL-94 Ratings of the PA6/PE/SAMH Ternary Composites

Composite	Processing procedure	LOI value (%)	UL94 rating (3.2 mm)
PESA		32	V-1
PASA		41	V-0
PAEAM1	One-shot method	30	V-1
PAEAM2	Master-batch method	33	V-0

The PA6/LLDPE blends flame-retarded by SAMH were effective for dripping resistance. This have been because of two aspects: on the one hand, LLDPE increased the melt viscosity of the composite, and on the other hand, SAMH particles tended to be coated by the high-viscosity LLDPE, and the coated SAMH engendered less influence on the degradation of PA6. Because of the incompatibility between the polar PA6 and nonpolar LLDPE, PE-*g*-MAH was chosen as a compatibilizing agent to provide a much stronger interaction of PA6 and LLDPE. As for the PA6 composite with 30 wt % SAMH, a loading of 15 wt % LLDPE and 5% PE-MAH (short for 20 wt % PE) could withstand the dripping to attain a UL94 V-0 rating at a 3.2-mm thickness. In addition, the flame-retardance properties quite depend on the dispersion of the flame-retardant particles in the polymer matrix,[13] and a master-batch processing method aids the dispersion of inorganic particles in the polymer matrix.[14] With PA6/PE/SAMH held at a 50/20/30 weight ratio, the master-batch method and a one-shot method were used to prepare the ternary composites. The LOI and UL-94 test results of the two corresponding PA6/PE/SAMH ternary composites PAEAM1 and PAEAM2 are compared with PESA and PASA in Table I.

The LOI value of PAEM2 was 33%, whereas that of PAEM1 was 30%. Ignited PAEAM2 specimens self-extinguished in air with a very short average combustion time and passed the V-0 rating, whereas

TABLE II
Mechanical Properties of PA6, LLDPE, and Their Binary and Ternary Composites

Name	Tensile strength (MPa)	Elongation at break (%)	Notched impact strength (J/m)	Flexural strength (MPa)
PA6	52.2	60	60	65.8
PASA	83.2	1	34	129.2
LLDPE	10.0	500	600	9.5
PESA	12.7	78	260	20.2
PAEAM1	48.5	7	42	41.6
PAEAM2	43.8	2	35	56.4

PAEAM1 specimens only provided a V-1 rating at a 3.2-mm thickness with a longer combustion time. Therefore, the ternary composite from the master-batch method was proven to be more efficient in suppressing the flammability than that produced by one-shot method. During UL94 testing, both PAEAM1 and PAEAM2 specimens did not drip; this indicated that LLDPE indeed played a critical role of resisting the dripping.

Mechanical properties

The mechanical properties of PA6, LLDPE, and their composites are listed in Table II. Compared to the pure PA6, PASA exhibited an increase of 59.3% in tensile strength and an increase of 96.4% in flexural strength, whereas the notched impact strength decreased by 46.7%, and the elongation at break decreased more evidently. This manifested that SAMH reinforced PA6 at the expense of fracture toughness. A similar reinforcing phenomenon was observed for PESA. For the two ternary composites, PAEAM2 showed a lower elongation at break and notched impact strength relative to PAEAM1 but exhibited a 35.6% higher flexural strength than PAEAM1. Under melt processing conditions, the degradation of PE generally occurred by crosslinking and chain scission reactions, which induced a poorer toughening of PAEAM2 via two extrusion.[15] Their difference in tensile strength is smaller. Although the increases for PAEAM2 in the elongation at break (2% vs 1%) and notched impact strength (35 vs 34 J/m) were inconspicuous, both ternary composites displayed an improvement in toughness over a flame-retarded binary PASA because of a lower SAMH loading with a deterioration in rigidity due to the addition of a soft LLDPE.

Morphological analysis of the impact-fractured surface

Morphology of the impact-fractured surface

The SEM morphologies of the impact-fractured sections of PASA and PESA are shown in Figure 1. As shown in Figure 1(a), the dispersion of SAMH particles was homogeneous, and most particles were embedded in the PA6 matrix, which indicated a stronger affinity between the SAMH particles and PA6 polymer. As shown in Figure 1(b), a portion of the SAMH particles were located in the LLDPE matrix; the other particles, coated by a thin LLDPE layer with a 1–5 μm diameter, emerged on the surface of the matrix, and the dispersion of SAMH was less uniform than in the PA6 matrix. Some SAMH particles maintained their original spherical shape with 0.5–1 μm diameter, as shown in Figure 2, which revealed a poorer affinity of SAMH to LLDPE than to PA6.

The feed formulation of PAEAM1 and PAEAM2 was the same, and the differences in the flame retardance and mechanical properties between the two composites were aroused by the different microstructures of the composites, such as the dispersion of SAMH particles and phase uniformity. The SEM morphologies of the impact-fractured sections of PAEAM1 and PAEAM2 are compared in Figure 3. The processing procedures gave rise to a wide range of variations in the blend phase boundary of the composites at a fixed composition. For PAEAM1, an evident two-phase PA6/PE structure with a

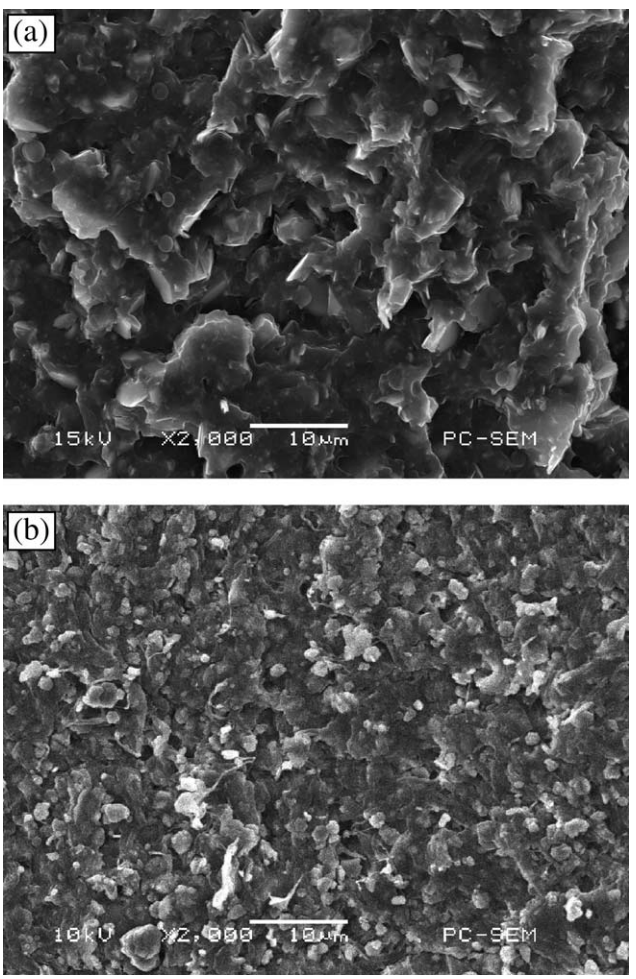

Figure 1 SEM micrographs of impact-fractured sections of (a) PASA and (b) PESA.

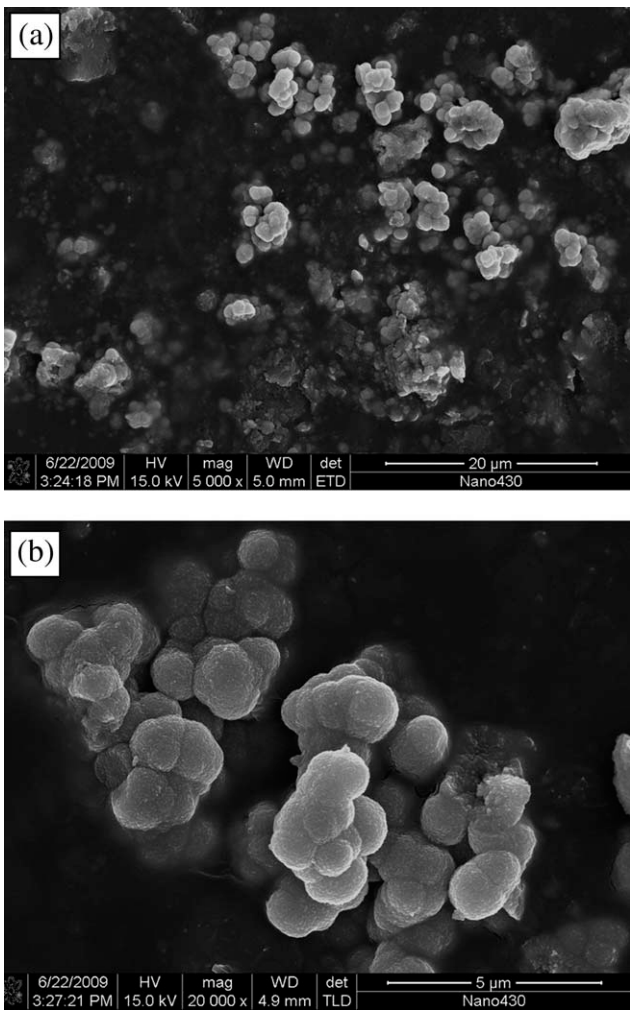

Figure 2 SEM micrographs of SAMH particles at different magnifications.

droplet/matrix morphology was observed, and LLDPE in a spherical shape was drawn out during sudden impacts; the reserved cavities could be clearly discerned. The SAMH particles were principally located in the PA6 phase, and a minority of them was located in the PE phase. PAEAM2 from the master-batch method had a morphology that resembled that of a binary composite. The phase interface between LLDPE and PA6 almost disappeared, and the SAMH fillers were evenly dispersed in a cocontinuous PA6/PE polymer matrix.

Morphology analysis

The ternary composites comprised two immiscible thermoplastic PA6 and LLDPE and one reinforced SAMH filler with a PE-*g*-MAH compatibilizing agent. Modification of the interfacial properties was implemented with surface-modified metal hydroxides and PE-*g*-MAH compatibilizer. SAMH containing an organic coating by the chemical bonding of ATH and MH with H_3BO_3, γ-PSi, and diphenylsilanediol exhibited some interaction with PA6 and LLDPE, as shown in Figure 1. For PAEAM1 and PAEAM2 at a fixed composition, the morphology contrast was mainly evoked by the blending procedure. Inorganic fillers are preferentially absorbed by a higher affinity polymer component in a blend.[16,17] As for PAEAM1, because four kinds of substances (PA6, LLDPE, PE-*g*-MAH, and SAMH) were synchronously compounded and extruded, the SAMH fillers were liable to be attracted by PA6 with the high specific surface energy to minimize the total interfacial energy of the ternary system, and the dispersion of the fillers was mostly governed by the polar interaction of PA6. Thus, filler particles were selectively located in the close-up of the PA6 phase, and a droplet/matrix coarsening morphology was formed, as displayed in Figure 3(a).

As far as PAEAM2, the SAMH particles were encapsulated by LLDPE and PE-*g*-MAH layer in the first step. The coated layer of SAMH particles contained PE-*g*-MAH, whose PE side was tangled with the LLDPE polymer chain, and the anhydride group reacted with PA6. The strong interaction between PA6 and PE-*g*-MAH was enough to allow for the

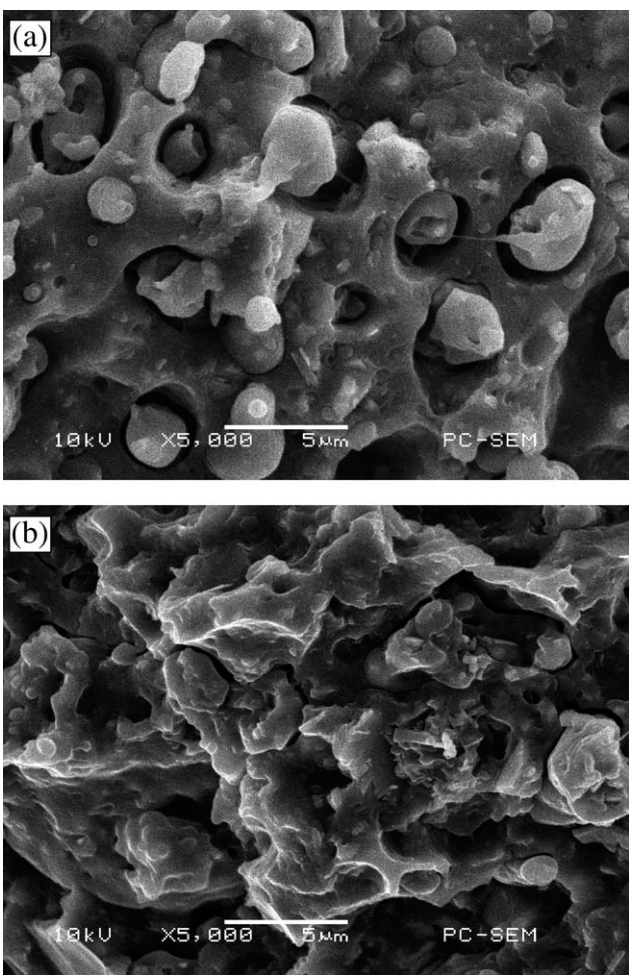

Figure 3 SEM micrographs of impact-fractured sections of (a) PAEAM1 and (b) PAEAM2.

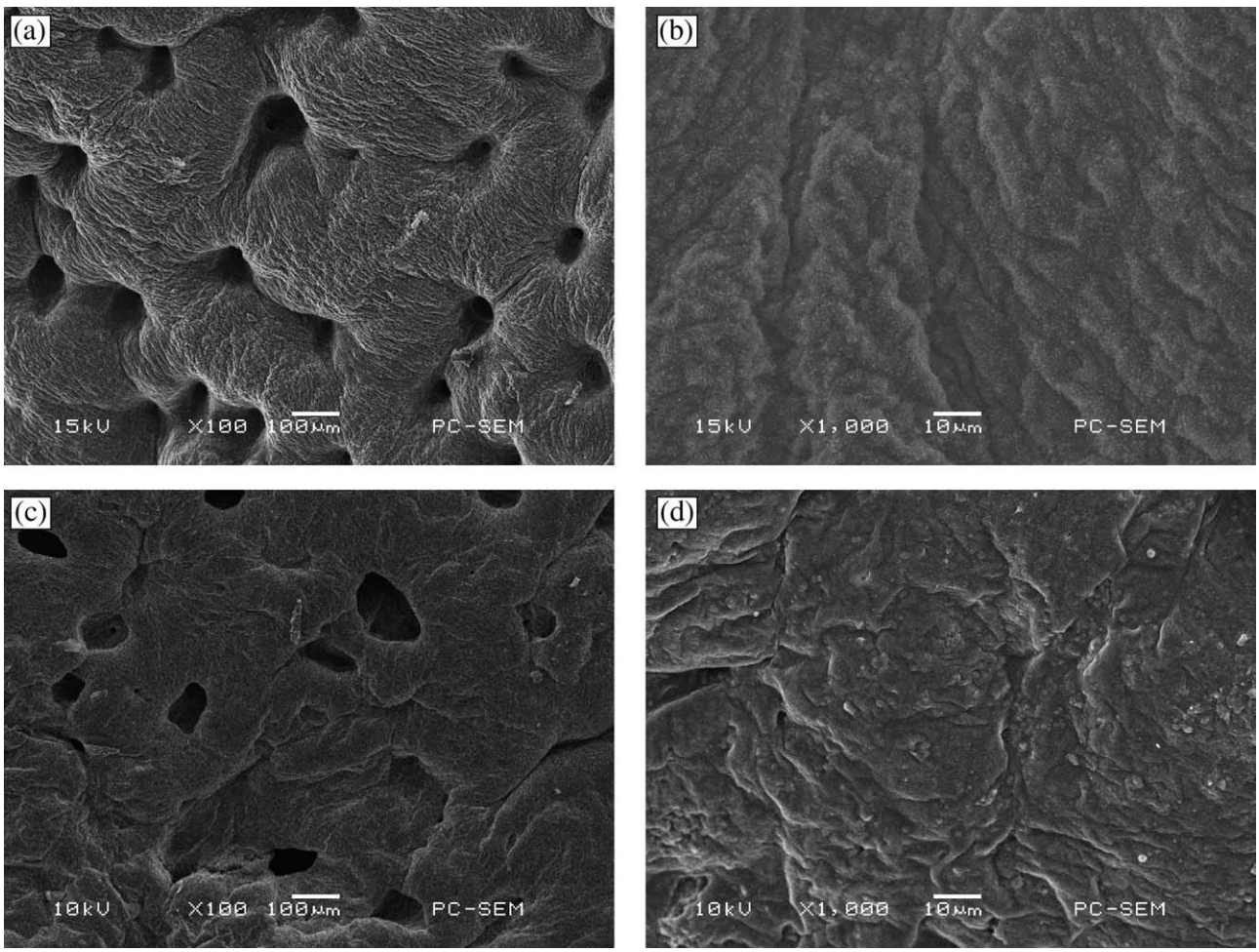

Figure 4 SEM images of residues after the first ignition of (a,b) PAEAM1 and (c,d) PAEAM2 at different magnifications.

formation of a cocontinuous PA6/PE phase in the second step. At the same time, the SAMH fillers, with a more optimal affinity to PA6, also promoted the continuity of this phase.[18] As a result, the SAMH particles were uniformly dispersed in the cocontinuous PA6/PE matrix, and a 35.6% higher flexural strength of PAEAM2 than PAEAM1 was obtained.

Morphology of the residue surfaces

Externally, there was a large difference between the residues of PAEAM1 and PAEAM2 in the UL 94 vertical burning tests. A tiny carbon black was covered in the burning section of PAEAM1, whereas the burning section of PAEAM2 was superficially scorched. The differences were clearly reflected in the SEM images of the residues of PAEAM1 and PAEAM2. Their SEM images after the first ignition are shown in Figure 4. A porous carbon layer was found for both PAEAM1 and PAEAM2, but the carbon layer structure of PAEAM2 was more compact than that of PAEAM1.

The flame retardance of ATH and MH could be interpreted as a condensed-phase action. Apart from a significant amount of water evolved into the flame, ATH and MH converted into a substantial amount of MgO and Al_2O_3 crystals to significantly decrease the heating rate of the polymer surface. After the second ignition, the carbon layer burned more completely. Somewhat different morphological appearances were observed in the SEM images of the residue after the second ignition, as shown in Figure 5. The residue of PAEAM1, shown in Figure 5(b), seemed to be composed of regular MgO and Al_2O_3 crystals from the decomposition of ATH and MH, which were loosely stacked together. An inferior flame-retardance property manifested that the kind of residue could not resist the transfer of air and heat. As shown clearly in Figure 5(d), platy and regular crystals in the residue of PAEAM2 clung firmly together to create a continuous vitreous protective layer. We believe that the polymer fragments from the pyrolysis of PA6 and PE counted for the cement of MgO and Al_2O_3 crystals. The good flame-retardance effect demonstrated that it could act as a physical barrier to stop flame penetration.

SEM/EDX analysis

The morphologies of the residues of PAEAM1 and PAEAM2 after the second ignition and the

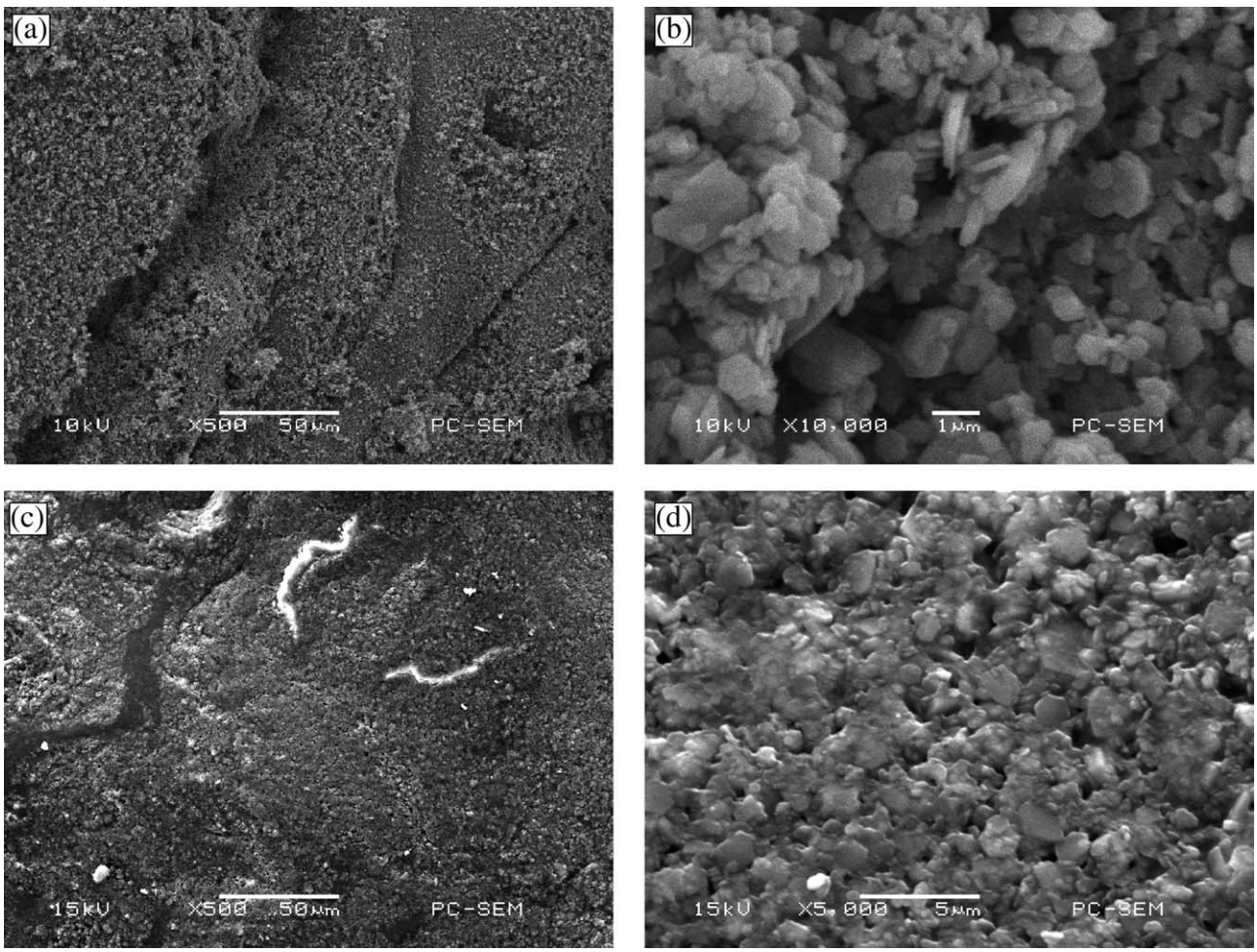

Figure 5 SEM images of residues after the second ignition of (a,b) PAEAM1 and (c,d) PAEAM2 at different magnifications.

corresponding element distribution obtained from SEM/EDX are displayed in Figure 6 and Table III. The boric acid component helped to form a glassy protective layer on the surface of burning polymer, but the boron element could not be detected by SEM/EDX because of the limits of the instrument. It was found that Mg, Al, C, and O built into the matrix structure, but their distribution was different in two kinds of residual carbon. The results in Table III demonstrate that very large amounts of MgO and Al_2O_3 were enriched and identified as a condensed phase. However, the O concentration in PAEAM2 seemed to be smaller than in PAEAM1, whereas the C concentration in PAEAM2 was higher. This was probably due to the favorable resistance to O_2 entrance of the PAEAM2 char layer. The data shown in Table III made clear the presence and accumulation of P and Si elements in the PAEAM2 residue. P was beneficial for the formation of a compact char layer during the burning of the polymer materials because of the formed phosphoric acid acting as a dehydrating agent. The presence of Si may have improved the thermal oxidative stability of the char layer.[19] We concluded that the complex action of ATH, MH, and the P, B, and Si elements interfered with the decomposition process of PA6 and PE and resulted in the formation of a thin glassy protective coating, which, in turn, lowered the oxygen diffusion and heat and mass transfer between the combustible gas and the condensed phase. Finally, the desired flame-retardance effect of PAEAM2 was achieved.

No P or Si was detected in different observed areas that looked homogeneous in the PAEAM1 residual carbon. Thus, we concluded that the inclusion of small amounts of P and Si elements into the char layer was key to the flame-retardance improvement of the ternary composites. The inherent distinction between PAEAM1 and PAEAM2 was in the dispersion of SAMH and the phase uniformity. The flame-retardance properties of a composite depend greatly on the dispersion of flame-retardant particles in the polymer matrix.[13] It is difficult for an uneven system to form a compact flame-resistant char shield containing B, P, and Si elements. Air and heat are prone to transfer through the less tenacious region to reduce the whole flame-retardance effect of

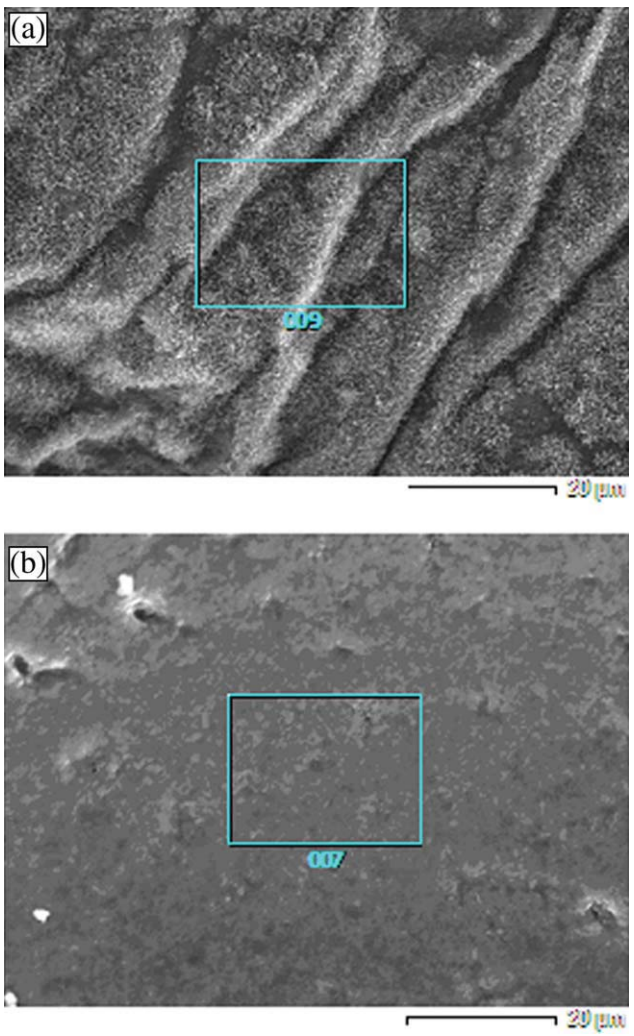

Figure 6 Morphologies of residues of the second ignition by SEM/EDX for (a) PAEAM1 and (b) PAEAM2. [Color figure can be viewed in the online issue, which is available at www.interscience.wiley.com.]

PAEAM1. A cocontinuous PA6/PE polymer host and a preferential dispersion of SAMH particles in the matrix of PAEAM2 lead to the formation of a highly flame-resistant char layer.

TGA

ATH started to decompose at approximately 250°C and MH at 340°C. Two composites were processed at 235°C, which was close to the stability limit of the ATH fillers but well within the capability of MH. The TGA curves of SAMH, PA6, LLDPE, PAEAM1, and PAEAM2 in a nitrogen atmosphere at a heating rate of 20°C/min are shown in Figure 7. The 1% weight loss temperature of SAMH was 233°C, and SAMH could withstand the processing temperature to be compounded with PA6/LLDPE. The pure PA6 exhibited a small weight loss in the range 90–200°C because of the absorption of physical water, then presented a one-step degradation process, and completed thermal degradation up to 550°C. LLDPE showed only a one-step degradation process in the range 403–500°C. There were 4.4 and 2.5% residues at 550°C for PA6 and LLDPE, respectively.

TABLE III
Elemental Distributions of the Residues of PAEAM1 and PAEAM2 After the Second Ignition by SEM/EDX

Formulation	Mg	Al	Si	P	C	O
PAEAM1	8.0	8.2	0	0	48.4	27.8
PAEAM2	12.6	4.7	0.9	1.2	52.3	18.8

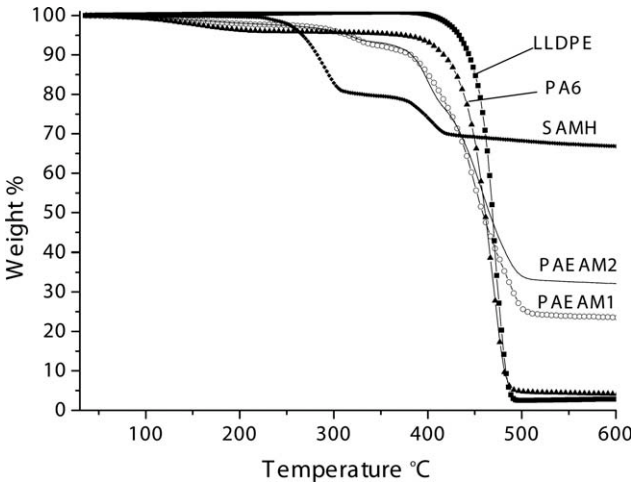

Figure 7 TG curves of (◆) SAMH, (▲) PA6, (■) LLDPE, (○) PAEAM1, and (—) PAEAM2 in N_2 at a heating rate of 20°C/min.

The degradation profiles of PAEAM1 and PAEAM2 were similar to that of PA6 before 200°C, and then both PAEAM1 and PAEAM2 proceeded to a three-step process, as shown in their differential thermogravimetry (DTG) curves (Fig. 8). However, the different maximum weight loss temperature (T_{max}) of each step indicated their different degradation processes. Weight losses of 9.0% of PAEAM1

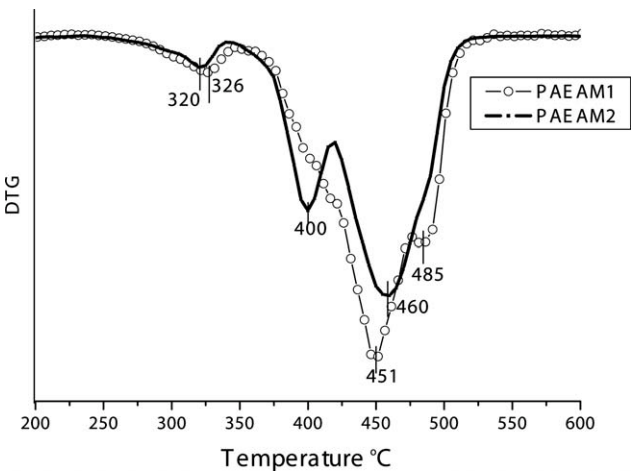

Figure 8 DTG curves of (○) PAEAM1 and (—) PAEAM2 in N_2 at a heating rate of 20°C/min.

and PAEAM2 occurred in the first step from 265 to 390°C because of the decomposition of ATH and MH from SAMH, which was close to 10% of the theoretical weight loss of SAMH; this indicated the decomposition completion of a majority of SAMH. Before 390°C, the weight loss trend of PAEAM2 was the same as that of PAEAM1, and the T_{max} values of PAEAM1 and PAEAM2 were 326 and 320°C, respectively. A noteworthy observation was that PAEAM2 degraded more quickly than PAEAM1 and formed one evident step with a 15.6% weight loss in the temperature range of 390–430°C, whereas PAEAM1 formed no single step. The appearance of the second step of PAEAM2 with T_{max} at 400°C implied the occurrence of a remarkable variation in the degradation modes of PA6 and PE. The following third degradation rate of PAEAM2 in the temperature range 430–510°C with T_{max} at 460°C, attributed to the PA6/PE polymer chain breakdown, was slower than that of PAEAM1, whereas PAEAM1 exhibited two obvious degradation steps in the range 430–510°C, and the T_{max} values were 451 and 485°C, respectively. The third degradation step of PAEAM1 in the temperature range 475–510°C may have been due to the degradation of PE; this indicated that the presence of several flame retardants had a small effect on the degradation process of PE. As a result, PAEAM1 and PAEAM2 degraded with 32.6 and 23.9% residue at 550°C, respectively. The residue of 30% SAMH, calculated according to the full decomposition of ATH (the residue by 65%) and MH (the residue by 70%), should have been 20%, and the degradation of PA6/LLDPE/PE-*g*-MAH yielded about 2.7% ash residues. The solid residue of several materials simply added up to 22.7%, and a 23.9% residue of PAEAM1 was close to the value; this indicated less charring of PA6 and PE degradation. A 9.9% redundant portion of PAEAM2 should have mainly originated from the charring of the PA6 and PE polymer. The assumption of PA6 and PE fragments cementing MgO and Al_2O_3 crystals in the SEM image analysis of PAEAM2 residue was, to some degree, confirmed by the high charring rate. We concluded from these results that an improved flame retardance of the ternary composites was combined with a higher charring of PA6 and PE degradation.

CONCLUSIONS

Three synergistic co-additives, boric acid, γ-PSi, and diphenylsilanediol coupling agents, were jointly introduced into the mixture of ATH and MH (2 : 1 by weight ratio) in a surface-modified process. The surface-modified metal hydroxides (SAMHs) were more acceptable for application in the PA6/LLDPE blend with a PE-*g*-MAH compatibilizer. The final flame-retardance and mechanical properties of PA6/PE/SAMH at a 50/20/30 weight ratio were correlated with the processing procedures. The ternary composite by a master-batch method (PAEAM2) passed to a UL94 V-0 rating at a 3.2-mm thickness with a 33% LOI value, whereas the same component ternary composite by a one-shot method (PAEAM1) only passed to a UL94 V-1 rating at a 3.2-mm thickness with a 30% LOI value. Two composites displayed an improvement in the toughness over a flame-retarded PA6/SAMH binary composite at a 50/50 weight ratio. The SEM morphologies of the impact-fractured section of PAEAM2 indicated that the SAMH fillers were evenly dispersed in a cocontinuous PA6/PE polymer matrix. The morphologies of the residue of PAEAM2 after the second ignition and corresponding elemental distribution from SEM/EDX exhibited a highly flame-resistant char shield containing P and Si elements. TGA showed that the higher solid residue rate of PAEAM2 was efficiently promoted by the charring of PA6 and PE. The phase continuity and SAMH filler uniform dispersion in the ternary composites were responsible for the char shield and solid residue rate, which induced a high flame retardance.

References

1. Valenza, A.; Geuskens, G.; Spadaro, G. Eur Polym J 1997, 33, 957.
2. Catano, L.; Albano, C.; Karam, A.; Perera, R.; Silva, P. Macromol Symp 2007, 257, 147.
3. Malchev, P. G.; Vos, G. D.; Norder, B.; Picken, S. J.; Gotsis, A. D. Polymer 2007, 48, 6294.
4. Su, Z. P.; Jiang, P. K.; Wei, P.; Wang, G. L.; Zhang, Y. J Appl Polym Sci 2005, 96, 162.
5. Rothon, R. N.; Hornsby, P. R. Polym Degrad Stab 1996, 54, 383.
6. Du, L. C.; Qu, B. J.; Zhang, M. Polym Degrad Stab 2007, 92, 497.
7. Nachtigall, S. M. B.; Miotto, M.; Schneider, E. E.; Mauler, R. S.; Forte, M. M. C. Eur Polym J 2006, 42, 990.
8. Du, L. C.; Qu, B. J.; Xu, Z. J. Polym Degrad Stab 2006, 91, 995.
9. Braun, U.; Schartel, B.; Fichera, M. A.; Jager, C. Polym Degrad Stab 2007, 92, 1528.
10. Kong, X. J.; Liu, S. M.; Zhao, J. Q. J Cent South Univ Technol 2008, 15, 779.
11. Li, Y. C.; Chen, G. H. Polym Eng Sci 2007, 47, 882.
12. Oliver, S.; Luckas, H. J.; Sandra, R. PCT Pat. WO 2005005519 (2005).
13. Samyn, F.; Bourbigot, S.; Jama, C.; Bellayer, S.; Nazare, S.; Hull, R.; Fina, A.; Castrovinci, A.; Camino, G. G. Eur Polym J 2008, 44, 1631.
14. Zoukrami, F.; Haddaoui, N.; Vanzeveren, C.; Sclavons, M.; Devaux, J. Polym Int 2008, 57, 756.
15. Al-Malaika, S.; Peng, X.; Watson, H. Polym Degrad Stab 2006, 91, 3131.
16. Fisher, I.; Siegmann, A.; Narkis, M. Polym Compos 2002, 23, 34.
17. Persson, A. L.; Bertilsson, H. Polymer 1998, 39, 5633.
18. Persson, A. L.; Schreiber, H. P. J Polym Sci Part B: Polym Phys 1997, 35, 2457.
19. Ravadits, I.; Toth, A.; Marosi, G.; Marton, A.; Szep, A. Polym Degrad Stab 2001, 74, 419.